Detection of Somatic DNA Recombination in the Transgenic Mouse Brain

MASAO MATSUOKA, FUMIKIYO NAGAWA, KENJI OKAZAKI, LINDA KINGSBURY, KAZUYA YOSHIDA, URS MÜLLER, DAVID T. LARUE, JEFFERY A. WINER, HITOSHI SAKANO

A DNA construct containing the bacterial β-galactosidase gene (*lacZ*) was used to study somatic DNA recombination in the transgenic mouse brain. Recombination-positive areas of the adult brain were stained blue with X-gal, a substrate of β-galactosidase. Blue-colored cells appeared soon after birth, and continued to emerge in postnatal tissue. Staining was prominent in sensory as opposed to motor regions of the brain, and was present in more than 70 discrete areas of the nervous system. The possibility of DNA rearrangement is discussed with respect to the development of the central nervous system.

THE BRAIN, LIKE THE IMMUNE SYSTEM, RECOGNIZES AND memorizes many different external signals. Comparison of the immune system with the nervous system yields interesting parallels (*1*). An increasing number of examples are known for cell surface markers and differentiation factors that are found in both systems (*2–4*). Recently, it was found that the RAG-1 gene, which is necessary for the activation of recombination in lymphocytes (*5*), is transcribed in the brain (*6*). However, it remains to be determined whether the RAG-1 transcription in the brain is indicative of somatic gene rearrangement or of other events, such as DNA repair.

In the mammalian immune system, somatic DNA recombination is instrumental in generating functional immunoglobulin (Ig) and T cell receptor (TCR) genes. This recombination, known as V-(D)-J joining (*7–9*), generates a diversity of receptor genes by combining multiple gene segments (V, variable, D, diversity, J, joining), and by modifying the junctional sequences (*9–11*). In the antigen receptor genes, DNA rearrangement is also an effective mechanism for activating a particular member of a multigene family, bringing the promoter and enhancer elements into close proximity (*12, 13*). This type of gene activation mechanism may be in operation in other biological systems when the fate of cells is being determined. As first proposed for Ig genes (*14*), DNA rearrangement also permits cells to generate an active gene whose protein product consists of two distinct domains, one with a variable interaction site for potential ligands and the other with a fixed biological function. Whether such gene rearrangement is restricted to the immune system, or can occur in other tissues was the question addressed by this study.

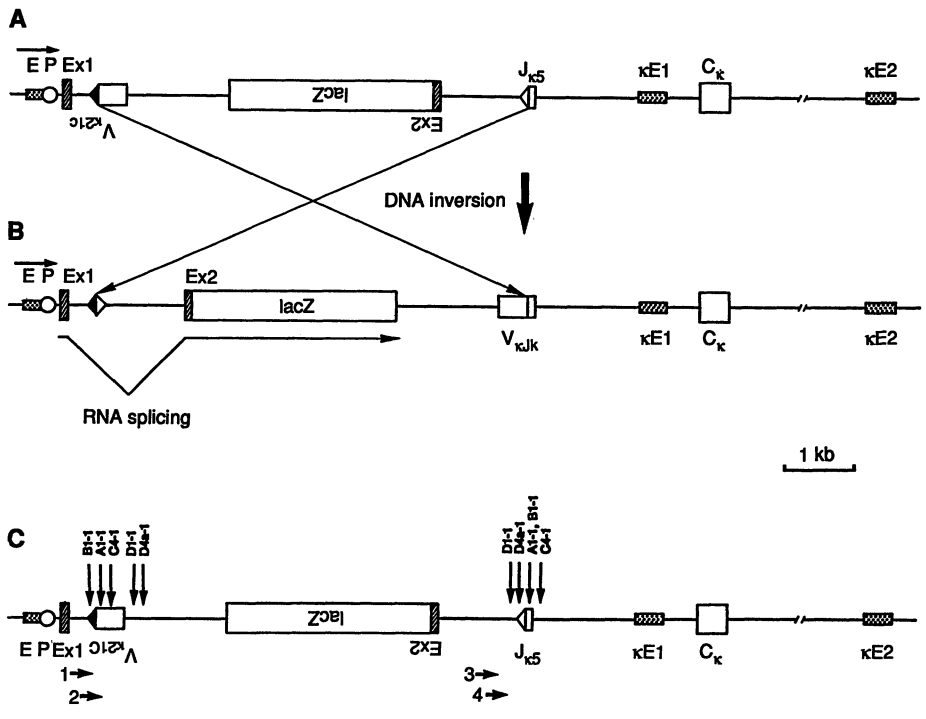

Fig. 1. Structure of the recombination reporter gene. The recombination substrate was constructed in plasmid pUC18 as described (*16*). Structures of the reporter gene before (**A**) and after (**B**) the rearrangement are shown schematically. In the substrate, the bacterial β-galactosidase gene, *lacZ* was placed in an inverse orientation relative to the transcriptional direction of the chicken β-actin enhancer-promoter (EP) complex. The *lacZ* gene was flanked by two recombination signal sequences (indicated by triangles) of the mouse Ig $V_{\kappa21C}$ and $J_{\kappa5}$ segments (7). The *lacZ* gene, when inverted, was transcribed into pre-mRNA by transcription from the β-actin promoter. RNA splicing signals of the actin gene exons (Ex1 and Ex2) were used to remove the extra sequence surrounding the signal junction (fused triangle). (**C**) Recombination breakpoints identified in brain cells. Recombination sites were determined by DNA sequencing (Fig. 3) after PCR amplification (*22*). The outer primers 1 and 3 were used in the Southern (DNA) blotting (Fig. 2). Inner primers, 2 and 4, were used in the second round of PCR amplification for DNA sequencing. Positions of primers are shown by horizontal arrows (5′ → 3′). Recombination breakpoints identified in brain cells are indicated by downward arrows on the map with names of the DNA clones.

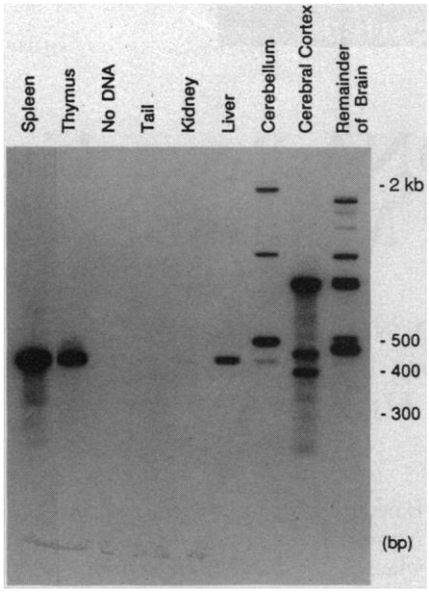

Fig. 2. Southern analysis of DNA rearrangements in the transgenic reporter gene. Nucleotide sequences at the signal junction were amplified with DNA samples (5 μg each) from spleen, thymus, liver, kidney, tail and brain. Primers used in the PCR amplification (*22*) were oligonucleotides 1 and 3 in Fig. 1C. Unrearranged DNA did not amplify because of the tandem orientation of the primers. After 35 cycles of amplification, the PCR products (one-twentieth of each) were separated in an agarose gel (2 percent) and analyzed by Southern blotting. The 5′-$J_{\kappa 5}$ sequence (Sph I–Pst I) was used as a hybridization probe.

To analyze DNA rearrangement at different stages of fetal and neonatal development, we generated transgenic mice with a recombination reporter gene. The substrate contained the bacterial β-galactosidase gene *lacZ* and two recombination signal sequences (RSS's) (*7, 15*). In the transgenic mice, we found that not only lymphatic tissues, but also many parts of the brain, were stained selectively with X-gal, which detects the expression of *lacZ*.

Detection of recombination by X-gal staining. The reporter gene introduced into transgenic mice (*16*) contained the promoter-enhancer complex of the chicken β-actin gene (*17*), the bacterial *lacZ* gene lacking its promoter, and RSS's of mouse Ig V_κ and J_κ segments (*7*) (Fig. 1A). In the construct, the *lacZ* gene is placed in the opposite orientation relative to the actin promoter. Since the two RSS's are situated in a tandem orientation, rearrangement results in DNA inversion relocating the *lacZ* gene in the correct transcriptional orientation (Fig. 1B). Activation of *lacZ* can then be detected by staining cells with X-gal, a substrate of β-galactosidase (β-gal).

The β-actin promoter-enhancer complex was chosen in order to obtain proper expression of *lacZ* wherever it was activated, regardless of tissue type. If the site-specificity of recombination in the brain were not as strict as in V-(D)-J joining in lymphocytes, joining sites could vary within a DNA region of a few kilobases, as it does in Ig switch recombination (*9*). For this reason, sufficient space was maintained in front of the *lacZ* gene to allow for flexibility of the recombination site. This ensured that part of the *lacZ* coding sequence or even the promoter-enhancer complex would not be deleted during the recombination process. To adjust for flexible joining we introduced two RNA splice sites, so that the extra sequence could be removed by RNA splicing (Fig. 1B).

Transgenic mice were generated by injecting the reporter gene into fertilized oocytes (*18, 19*). Two transgenic founders were obtained, one (No. 1) containing about 15 copies of the construct and the other (No. 2) containing a few copies. The DNA rearrangement was examined first in lymphocytes by staining cells with X-gal (*20*). The frequencies of blue-colored cells in the adult spleen were 10^{-3} to 10^{-4} in the No. 1 mouse and 10^{-2} in the No. 2 mouse. Colored cells were less common in the thymus. No blue lymphocytes were found in nontransgenic animals. When the transgenic splenocytes were cultured with a mitogen lipopolysaccharide (LPS), the frequency of colored lymphocytes was about ten times greater. Bone marrow cells from the No. 1 founder were analyzed in long-term bone marrow culture (LTBM). When the cells were cultured for 4 weeks

Table 1. A summary of β-gal-stained brain structures in the transgenic mouse brain. Areas are arranged in functional categories for analytical purposes. Two observers at a dual viewing microscope studied 50-μm-thick, transverse sections that had been reacted with X-gal and counterstained with neutral red. Architectonic regions were determined by reference to standard brain atlases. Concordance between the observers was required for inclusion in the table and for estimates of the intensity of labeling. Areas of intense β-gal activity: (i) granule cell layer of cerebellar cortical lobes IX and X, (ii) pyramidal cell layer of hippocampus, (iii) deep layers of perirhinal and entorhinal cortex, (iv) inferior olive, (v) amygdaloid nuclei, (vi) spiral ganglion cells. Areas of pale or sparse β-gal activity: (i) Purkinje cell layer of cerebellum, lobes IX and X, (ii) layer IV of primary visual cortex, area 17, (iii) pretectum, (iv) medial geniculate body, (v) ventral horn of spinal cord.

Pain and temperature

1. cervical spinal cord (laminae I–III)
2. raphe nuclei (rostral linear nucleus)
3. spinal trigeminal nucleus (caudal part)

Visual system

1. superior colliculus (superficial layer)
2. nonprimary visual cortex
3. primary visual cortex (layer IV only)
4. pretectum
5. suprageniculate nucleus
6. lateral posterior nucleus
7. accessory optic system (medial terminal nucleus)
8. Edinger–Westphal nucleus

Reticular formation

1. lateral reticular nucleus

Limbic and autonomic system

1. nucleus solitarius
2. retrosplenial granular cortex
3. retrosplenial agranular cortex
4. piriform cortex
5. amygdalopiriform transition area
6. dorsomedial thalamic nucleus
7. hypothalamus (ventromedial part)
8. corticomedial amygdaloid nucleus
9. anterior cortical amygdaloid nucleus
10. laterodorsal thalamic nucleus
11. central lateral thalamic nucleus
12. anteroventral thalamic nucleus
13. ventral presubiculum
14. medial preoptic area
15. agranular insular cortex
16. cingulate cortex
17. islands of Calleja
18. nucleus accumbens septi
19. lateral orbital cortex
20. infralimbic cortex
21. ventral orbital cortex

Motor control (conscious)

1. facial motor nucleus
2. cervical spinal cord (ventral horn, C_1–C_4)
3. cortical motor areas

Somatic sensory system

1. nucleus gracilis
2. nucleus cuneatus
3. medial lemniscus
4. ventrobasal complex of thalamus
5. parietal cortex (layer Va)
6. anterior parietal cortex

Auditory system

1. cochlear ganglion cells
2. posteroventral cochlear nucleus
3. dorsal cochlear nucleus
4. inferior colliculus (dorsal cortex)
5. inferior colliculus (lateral nucleus)
6. brachium of the inferior colliculus
7. medial geniculate body
8. primary auditory cortex
9. secondary auditory cortex
10. suprageniculate nucleus

Hippocampus and related centers

1. posterior entorhinal cortex
2. presubiculum
3. entorhinal cortex
4. subiculum
5. dentate gyrus (polymorphic layer)
6. pyramidal cell layer of hippocampus
7. perirhinal cortex
8. amygdala (basolateral part)
9. parasubiculum
10. dentate gyrus (hilum)
11. fimbria

Olfaction

1. nuclei of the basal olfactory tract
2. olfactory tubercle
3. posterior olfactory nucleus (anterior part)
4. anterior olfactory nucleus
5. accessory olfactory bulb
6. piriform cortex

Motor control (subconscious)

1. paraflocculus (ventromedial part)
2. cerebellar granule cell layer of lobes IX and X
3. cerebellar cortex (Purkinje cell layer)
4. pontine nuclei
5. superior colliculus (deep layers)
6. substantia nigra (*pars compacta*)
7. interpeduncular nucleus
8. caudoputamen
9. globus pallidus

M. Matsuoka, F. Nagawa, L. Kingsbury, K. Yoshida, and H. Sakano are in the Division of Immunology and D. T. Larue and J. A. Winer are in the Division of Neurobiology, Department of Molecular and Cell Biology, University of California, Berkeley, CA 94720. K. Okazaki was at the Tsukuba Life Science Center, RIKEN, Ibaraki 305, and is currently at the Institute of Life Science, Kurume University, Kurume, Fukuoka 830, Japan. U. Müller is at the Basel Institute for Immunology, 487 Grenzacherstrasse, CH-4005 Basel, Switzerland.

Fig. 3. Nucleotide sequences around recombination breakpoints in the transgenic reporter gene. In order to sequence rearranged DNA, the fragments detected by Southern blotting (Fig. 2) were cloned into the sequencing vector pBluescript II KS(+) (Stratagene). Before cloning, DNA's were amplified with the second set of primers (2 and 4 in Fig. 1C) to eliminate nonspecific amplification (*22*). Sequences are shown for lymphocyte (**A**) and brain cell (**B**) DNA's. Two recombination signal sequences (RSS's) are joined in a head-to-head fashion in spleen (S) and thymus (T) clones. In brain cells, joining appears to be far less precise. Predicted recombination sites are indicated by vertical lines. Rearranged sequences in the middle are compared with the unrearranged counterparts, $V_{\kappa 21C}$ and $J_{\kappa 5}$ (7). Identical residues between the rearranged and unrearranged sequences are indicated by colons (:). Conserved heptamer and nonamer sequences in RSS's are underlined. Names of the clones are shown at the right end of the sequence.

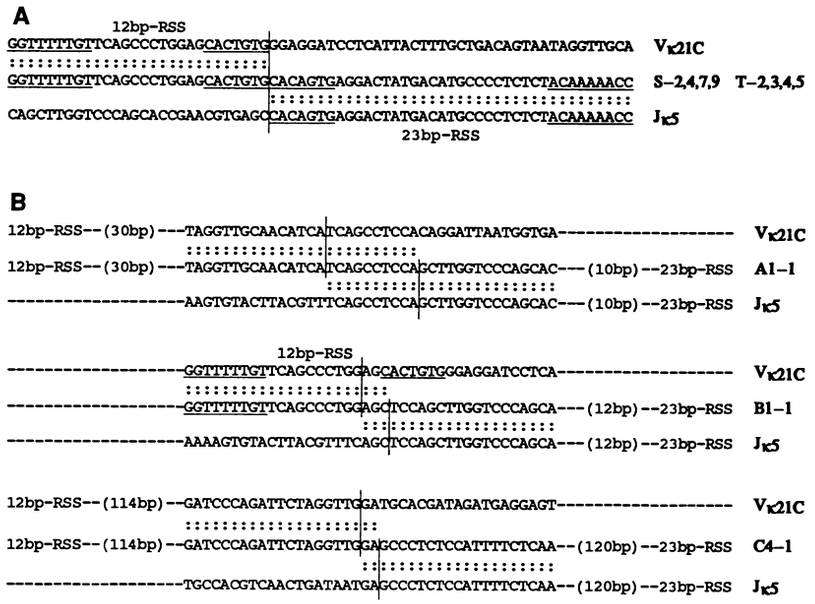

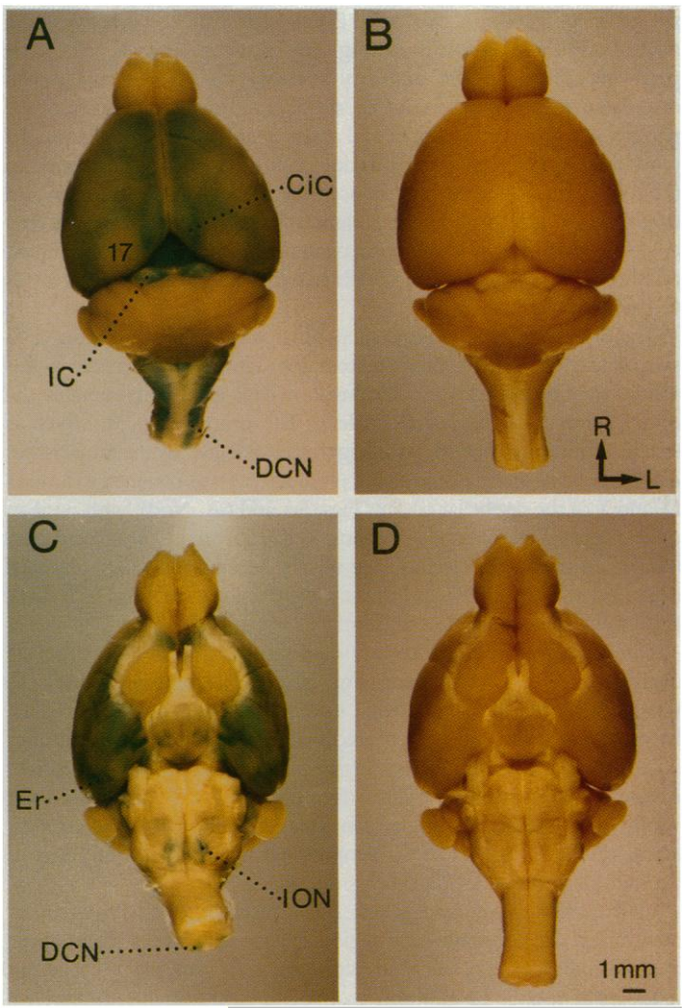

Fig. 4. X-gal staining of whole brains. (**A**) Superior view of transgenic mouse brain stained for β-gal activity. Staining is visible macroscopically in the inferior colliculus (IC), cingulate cortex (CiC) and dorsal column nuclei (DCN). (**B**) Control brain, nontransgenic littermate devoid of β-gal. (**C**) Inferior view of transgenic brain, showing the β-gal activity in the dorsal column nuclei (DCN), inferior olivary nucleus (ION), and entorhinal cortex (Er). (**D**) Nontransgenic control; R, rostral; L, lateral.

(*21*), blue-colored lymphocytes appeared at a frequency of 10^{-2}.

To confirm that *lacZ* activation was due to DNA recombination, we analyzed DNA samples from lymphatic organs and various other tissues (Fig. 2). The mice were perfused with phosphate-buffered saline (PBS) to eliminate residual lymphocytes from nonlymphatic organs. With the primers shown in Fig. 1C, DNA sequences surrounding the recombination junctions were amplified by polymerase chain reaction (PCR) (*22*). In this PCR procedure, unrearranged genes do not produce amplified DNA because of the tandem orientation of the primers. In the Southern (DNA blotting) analysis (Fig. 2), the sequence upstream of $J_{\kappa 5}$ was used as a hybridization probe. A discrete 400-bp band, which was expected for the signal junction, was detected in spleen and thymus. A faint 400-bp band was seen in the liver sample, which could have been due to residual lymphocytes. The rearranged band was not found in the DNA from the mouse tail or kidney. To our surprise, brain samples gave multiple bands, each of which differed in size from the 400-bp band.

Cloning analysis revealed differences in nucleotide sequences at recombination junctions in the rearranged DNA (Fig. 3). For the 400-bp fragment detected in lymphocytes, a typical signal junction was found, in which a 12-bp RSS and a 23-bp RSS were recombined in a head-to-head fashion (Fig. 3A). At the coding junction, recombined $V_{\kappa 21C}$ and $J_{\kappa 5}$ sequences were identified with nucleotide deletions, or sometimes additions. These results indicated that the recombination observed on the substrate in lymphocytes was similar to the joining found in the endogenous Ig and TCR genes. To study the nature of recombination in the brain, we cloned and sequenced the DNA bands that were amplified on the substrate (Fig. 3B). Compared to the signal junctions identified in lymphocytes (Fig. 3A), the joining in brain cells appeared to be far less precise (Fig. 1C).

Selective staining of specific brain regions by X-gal. For the study of β-gal activity in nonlymphatic tissues, 3-month-old animals were perfused (*23*), and various organs were stained with X-gal. Only in the brain and spinal cord was there a significant difference in staining between the transgenic and nontransgenic animals. In other tissues examined, such as lung and liver, no differences were apparent. Blue-colored cells became visible in transgenic brains (No. 1 and No. 2) within 30 minutes of incubation. In the nontransgenic brain, blue cells probably due to endogenous β-gal appeared only after prolonged incubation (24 hours). The endogenous activity was rather strong in some other tissues, such as kidney and artery. Since

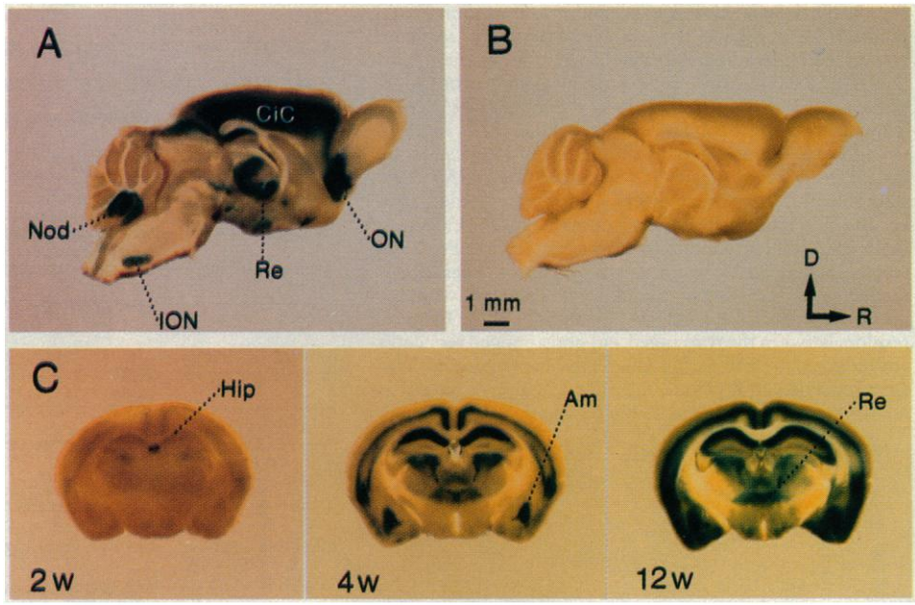

Fig. 5. β-gal activity detected in mouse brains. (**A**) Parasagittal view of transgenic brain stained with X-gal (*23*). Prominent β-gal activity was seen in the cerebellum (Nod), the inferior olivary nucleus (ION), cingulate cortex (CiC), nucleus reuniens (Re) and other thalamic nuclei, and in the forebrain olfactory nuclei (ON). (**B**) Nontransgenic control; D, dorsal; R, rostral. (**C**) Ontogenesis of β-gal expression in the transgenic mouse brain. Coronal sections from the telencephalon were stained with X-gal. Brains were isolated from transgenic mice at 2, 4, and 12 weeks (w) after birth. Sections were 500 μm thick. Staining is visible in the nodulus (Nod), hippocampus (Hip), amygdala (Am), and nucleus reuniens (Re).

the No. 2 founder did not yield offspring, the No. 1 strain was used for further analyses. After a 6-hour incubation with X-gal, the staining patterns of transgenic and nontransgenic brains were compared (Figs. 4 and 5). The β-gal activity was evident along virtually the entire neuraxis, including the upper levels of the cervical spinal cord and medulla (Fig. 4, A and C: DCN), the pons (Figs. 4C and 5A: ION), and cerebellum (Fig. 5A: Nod), and various thalamic nuclei (Fig. 5, A and C: Re); and it extended as far rostrally as the basal telencephalon (Fig. 5A: ON). A complete list of the stained structures observed appears in Table 1. Control brains were devoid of any β-gal activity (Figs. 4, B and D, and 5B).

In most cases, β-gal activity appeared as very fine dark blue dots 2 to 3 μm in diameter or, more rarely, as elongated, comma-shaped structures visible at the somatic poles of neurons (Fig. 6B). These structures imparted a blue cast to the cell or, if the β-gal activity was sufficiently intense, to an entire structure (Fig. 6B: ION; Fig. 6C: PCL). In plastic-embedded sections (1 to 2 μm thick), the staining was visible in the cytoplasm of neurons. While we cannot yet specify the exact locus of β-gal activity with respect to a particular organelle, its distribution was confined to certain nuclei, fiber tracts, or cortical layers, and it began or ceased abruptly with respect to their cytoarchitectonically defined borders with a high degree of precision.

The X-gal staining was not due to endogenous β-gal because other brain sections were stained by the avidin-biotin immunoperoxidase method in which rabbit antibodies to bacterial β-gal (anti-β-gal) were used. Fine dots resembling those previously detected with X-gal at the same loci were also stained with the anti-β-gal. For example, antibody staining within the hippocampus was observed in the transgenic brain, but not in the nontransgenic sample (Fig. 6D). Similar observations were made for other areas stained with X-gal, such as the cerebral cortex, in certain forebrain olfactory centers, thalamic nuclei, the superior and inferior colliculi, and the cerebellum.

A survey was made to determine specifically which nuclei and tracts were labeled. More than 70 areas were identified as β-gal positive (Table 1). Areas with only one or two dots of X-gal staining were not included. On gross examination, the β-gal activity appeared broadly dispersed in the brain. However, when labeled structures were grouped according to their functional and connectional affiliations, a pattern of order emerged (Table 1). For example, structures throughout the auditory system from spiral ganglion cells of cranial nerve VIII in the hindbrain to neurons in the auditory forebrain, expressed β-gal. However, β-gal activity was not distributed uniformly along any sensory, motor, or other pathway. Thus, in the auditory system, the β-gal activity was associated with some, but not all, spiral ganglion cells. This selective pattern was also seen in the dorsal and posteroventral cochlear nuclei (rhombencephalon), in the inferior colliculus (mesencephalon), in the medial geniculate body (diencephalon), and in the primary and nonprimary auditory cortex (telencephalon). Analogous patterns could be described for the somatic sensory, visual, motor control, and limbic systems, each of which has components at several levels of the neuraxis.

The β-gal activity in many centers often was specific to one subdivision or another. In the auditory system, for example, only certain nuclear subdivisions of the inferior colliculus showed β-gal activity, notably the dorsal cortex and the lateral nucleus. The central nucleus, which is essential for normal hearing, was largely free of β-gal. By the same token, in the cerebellar granule cell system, β-gal activity was confined to lobules IX and X of the cerebellar cortex (Figs. 5A and 6A: Nod), with none in other parts of the extensive granule cell domain in other cerebellar lobules. In contrast, in the inferior olivary nucleus and its subdivisions (Figs. 4C and 6B: ION) and in the amygdaloid nuclei (Fig. 5C: Am), β-gal staining was far more uniform.

The distribution and intensity of β-gal–positive cells progresses during postnatal development (Fig. 5C). In the newborn, blue cells were found only in the cerebellar nodulus and part of the thalamus. In the 2-week-old mouse, colored cells started to appear in other areas of the brain, such as the hippocampus and entorhinal cortex. At 4 weeks, practically the same distribution was obtained as in the adult, although the staining was less intense. The difference in intensity may simply reflect a progressive accumulation of β-gal in the cytoplasm of neurons expressing *lacZ*.

In the analysis of transgenes, one must consider the effect of integration sites on stage- and region-specific expression. To examine the possibility of the so-called promoter trap, analysis of different founders is useful. In addition to the No. 1 transgenic mouse, we studied another transgenic founder (No. 2). The β-gal expression in mouse No. 2 revealed X-gal stained cells in the spleen, spinal cord, and brain. Although further studies are needed to compare the No. 1 and No. 2 mice, detection of β-gal-positive cells in two transgenic brains indicates that *lacZ* expression is not an accidental event due to the promoter trap.

Recombination in the mouse nervous system. In the transgenic mouse specific regions of the brain were selectively stained with X-gal (Figs. 4 to 6). Immunocytochemical analysis revealed that X-gal stained areas were labeled with antibodies to bacterial β-gal (Fig. 6D). The nontransgenic tissue was devoid of labeling. Our data provide evidence that the staining of the transgenic brains was indeed due to the expression of exogenous *lacZ*. The X-gal staining pattern was stably inherited from the F_0 founder to transgenic F_1 and F_2 mice.

Although the distribution of the β-gal activity in the central nervous system is widespread, it is neither diffuse nor random. The main patterns of β-gal activity are as follows: (i) Staining was most apparent in phylogenetically ancient limbic or autonomic viscero-motor structures; (ii) it was more prevalent in sensory than in motor regions; (iii) it tended to favor secondary, rather than primary, sensory pathways; and (iv) it was often present in structures that are connected with one another and that are elements in a neural circuit. For documentation of the first point, we note that many phylogenetically older forebrain olfactory centers express β-gal; however, it was virtually absent in the olfactory bulb. Similar principles of continuity and discontinuity in β-gal distribution apply in the visual system, where the superior colliculus showed moderate activity while there was far less β-gal activity in the lateral geniculate body, and in its target, the visual cortex.

The second conclusion is that β-gal activity was more prevalent in sensory than in motor pathways. For example, the thalamic intralaminar nuclei, which are involved in autonomic, visceral, and pain sensibility (*24*) had a broad pattern of X-gal staining, while other nuclei that represent the special senses, which may be newer in evolution than systems for pain, temperature, and neurosecretion

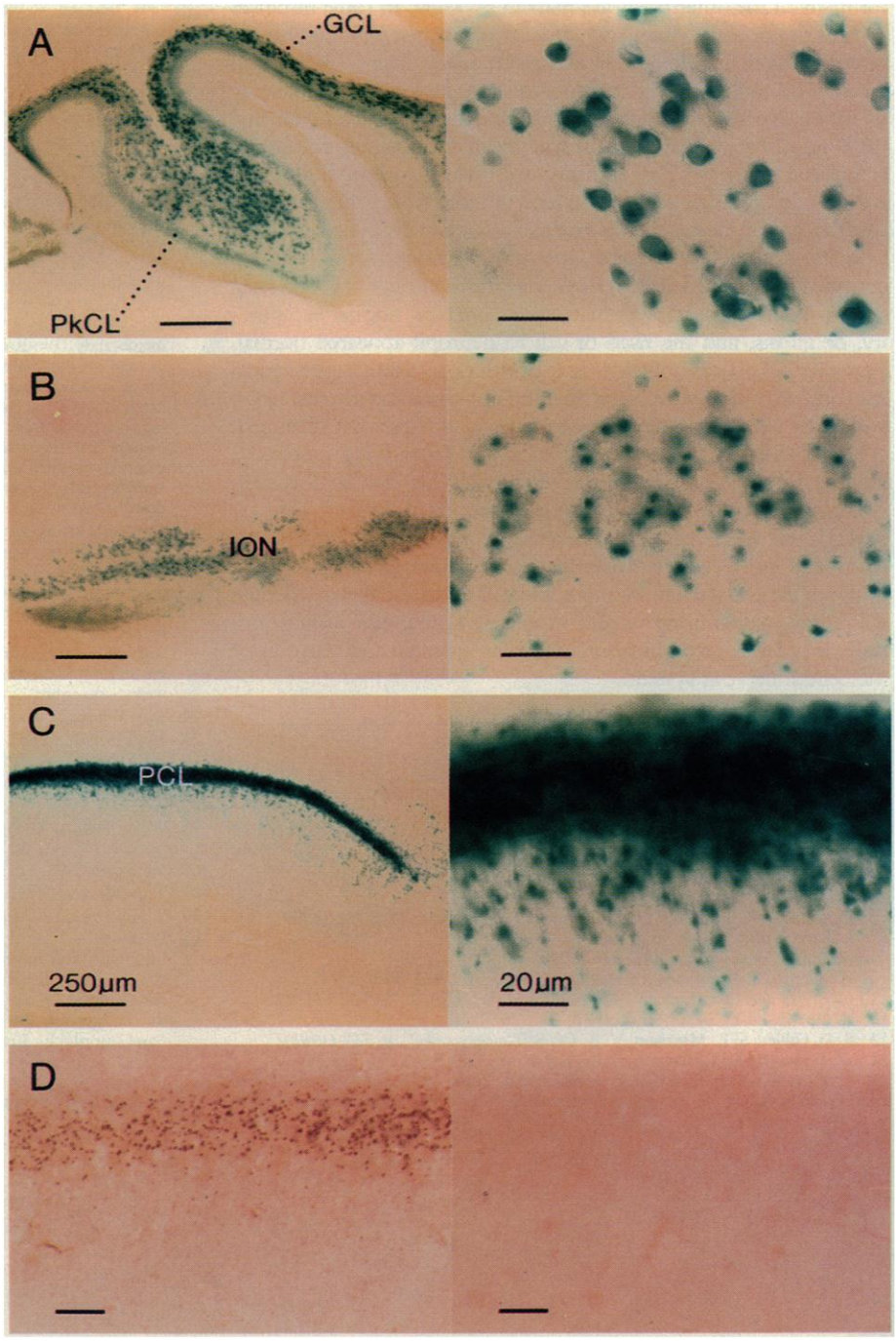

Fig. 6. Microscopic views of parasagittal brain sections. (**A**) The cerebellar nodulus. The β-gal activity is especially intense in the cerebellar granule cell layer (GCL). A faint blue tint is evident in the Purkinje cell layer (PkCL) of the cerebellar cortex. (**B**) The inferior olivary nucleus (ION). Punctate nature of the X-gal staining is seen at higher power [compare with cerebellar granule cells in (A)]. (**C**) The hippocampal CA1 region. The β-gal-positive cells are intense in the pyramidal cell layer (PCL). Scale bars in the left panels (lower magnifications) indicate 250 μm, while bars in the right panels (higher magnifications) indicate 20 μm. (**D**) Immunocytochemical analysis of brain sections. The hippocampus of the transgenic mouse (**left**) was stained with rabbit antibodies to bacterial β-gal (Cappel/Cooper Biomedical) and used at dilutions of 1:2000. Immunostaining was performed with the Vectastain ABC-kit from Vector Laboratories, Burlingame, California, according to the manufacture's recommendations. As a control, the hippocampus of a nontransgenic littermate (**right**) was stained with the antibodies. Scale bars in (D) indicate 20 μm.

(*25*), had a more limited distribution. Some cranial nerve motor nuclei were devoid of β-gal activity, while other motoneurons that were stained are part of the extrapyramidal system or related to subconscious motor processing (Table 1).

A third observation is that nonprimary sensory areas were preferentially stained with X-gal. Such centers often receive input from several modalities and have rather large receptive fields, whereas newer primary pathways receive input from one modality exclusively and have smaller receptive fields. Thus, in the medial geniculate body, the labeled subregions in the dorsal and medial divisions are connected mainly with subcortical limbic and motor forebrain centers (*26*), regions responsible for auditory-visceral reflexes and acoustic or visual modulation of motor output (*27*), and perhaps for reflexive postural adjustments essential in the spatial localization of sound. Neither pathway, however, is essential for frequency analysis or the detection of sounds (*28*). Analogous arguments can be made for many of the other pathways marked by X-gal. In some instances such as the primary visual and auditory cortex, the staining was far lighter than in limbic-dominated, presumably older, paleocortical areas. This is consistent with both the predominantly sensory distribution of β-gal and its affinity for older neural centers. Finally, β-gal activity was often found in synaptically interconnected parts of a sensory pathway. The auditory and visual pathways are thus labeled along much of their extent, although the intensity and distribution of the reaction is particular to each synaptic station.

In 50-μm-thick frozen or vibratome sections, there were no conspicuous pathological signs of classical neuronal degeneration, such as swelling, pyknosis, chromatolysis, pallor, nuclear eccentricity, or gliosis, and the ratio of cell to neuropil appeared normal. However, in plastic embedded 1.0-μm-thick sections, hippocampal neurons associated with X-gal staining appeared slightly shrunken, with their perikaryal membrane irregular and somewhat scalloped. Whether their shape after dehydration and embedding reflected a volume regulation phenomenon that could be due to the high concentration of β-gal remains to be investigated.

While the mode of DNA rearrangement is not yet known, our study has provided evidence that gene rearrangement may be involved in neonatal development. Identification and isolation of the rearranging genes in nerve cells should provide a new insight into the role of DNA recombination in the development and assembly of the central nervous system.

REFERENCES AND NOTES

1. N. K. Jerne, in *The Neurosciences*, G. C. Quarton, T. Melnechuk, F. O. Schmitt, Eds. (Rockefeller Univ. Press, New York, 1967), pp. 200–205.
2. P. J. Maddon *et al.*, *Cell* **47**, 333 (1986).
3. J. R. Parnes and T. Hunkapiller, *Immunol. Rev.* **100**, 109 (1987).
4. T. Yamamori *et al.*, *Science* **246**, 1412 (1990).
5. D. G. Schatz, M. A. Oettinger, D. Baltimore, *Cell* **59**, 1035 (1989).
6. J. J. M. Chun *et al.*, *ibid.*, p. 189.
7. H. Sakano, K. Hüppi, G. Heinrich, S. Tonegawa, *Nature* **280**, 288 (1979).
8. P. Early *et al.*, *Cell* **19**, 981 (1980).
9. H. Sakano *et al.*, *Nature* **286**, 676 (1980).
10. H. Sakano, Y. Kurosawa, M. Weigert, S. Tonegawa, *ibid.* **290**, 562 (1981).
11. F. W. Alt and D. Baltimore, *Proc. Natl. Acad. Sci. U.S.A.* **79**, 4118 (1982).
12. C. Queen and D. Baltimore, *Cell* **33**, 741 (1983).
13. S. D. Gillies, S. L. Morrison, V. T. Oi, S. Tonegawa, *ibid.*, p. 717 (1983).
14. W. J. Dreyer and C. Bennett, *Proc. Natl. Acad. Sci. U.S.A.* **54**, 864 (1965).
15. S. Akira, K. Okazaki, H. Sakano, *Science* **238**, 1134 (1987).
16. For construction of the reporter plasmid pκZ1, various DNA segments were assembled as follows. The 15-kb Eco RI fragment containing the mouse J_{κ}, C_{κ}, and enhancer elements (7) was subcloned into the Eco RI site of plasmid pUC18. The 2-kb region of the J_{κ}-C_{κ} fragment between the Eco RI and Ava I restriction sites was removed in order to delete four J_{κ} segments, $J_{\kappa 1}$ to $J_{\kappa 4}$. The 630-bp Sma I–Apa I fragment containing the chicken β-actin promoter, enhancer, and the first exon (*29*) was ligated to the 5′ end of the Ig κ fragment. In order to add the SV40 poly(A) site, the 850-bp Bgl II–Bam HI fragment of pSV2-dhfr (*30*) was ligated to the 3′ end of the *lacZ* gene. An RNA splicing acceptor site was attached to the 5′ end of the *lacZ* gene by ligating the 730-bp Apa I–Nco I fragment containing the 5′ portion of the actin gene exon 2. To the 3′ end of the *lacZ* construct, the 1.3-kb Bgl II fragment of the mouse Ig $V_{\kappa 21C}$ (7) gene was attached in the tandem transcriptional orientation. Finally, the 6-kb Apa I–Sal I V_{κ}–*lacZ* construct was inserted into the promoter-J_{κ} construct with the Sal I and Sma I sites in the multicloning region upstream from $J_{\kappa 5}$. On the substrate, the transcriptional orientation of *lacZ* is inverted compared with the transcriptional orientation of the β-actin promoter (Fig. 1).
17. N. Fregien and N. Davidson, *Gene* **48**, 1 (1986).
18. For microinjection, a 19-kb Eco RI fragment containing the recombination substrate was cleaved from the plasmid pκZ1 (*16*). The DNA was separated in an agarose gel, and electroeluted (Biotrap; Schleicher & Schuell). The DNA sample was dissolved in 10 mM tris-HCl (pH 7.5) and 0.25 mM EDTA at a concentration of 5 μg/ml. In order to make transgenic mice, a portion of DNA was microinjected into fertilized oocytes as described (*19*). Tail DNA (10 μg) from 4-week-old offspring was analyzed for the presence of the transgene by DNA (Southern) blotting. The *lacZ* sequence was used as a hybridization probe.
19. R. L. Brinster *et al.*, *Proc. Natl. Acad. Sci. U.S.A.* **82**, 4438 (1985).
20. J. R. Sanes, J. L. R. Rubenstein, J. F. Nicolas, *EMBO J.* **5**, 3133 (1986).
21. C. A. Whitlock and O. N. Witte, *Proc. Natl. Acad. Sci. U.S.A.* **79**, 3608 (1982).
22. Oligonucleotide primers used in the PCR amplification are as follows: (1) 5′-CGGGCTGTAATTAGCGCTTGGTTT-3′, (2) 5′-TTTCTGTGGCTGCGTGAAAGCCTT-3′, (3) 5′-AATGAGCCATTCCTGGCAACCTGT-3′, (4) 5′-GAAGATCCCCCAGAAAAGAGTCAG-3′. Genomic DNA was purified from various tissues that had been digested with proteinase K and extracted with phenol. Rearranged sequences were amplified by PCR with primers 1 and 3 (Fig. 1C) in a final volume of 100 μl. The Perkin-Elmer Cetus amplification kit was used under the following conditions: either 35 or 25 cycles of 20 s at 94°C, 20 s at 55°C, 30 s at 72°C. A portion (1/20) of each PCR reaction mixture was separated by electrophoresis in a 2 percent agarose gel and then transferred to Zeta-Probe membranes (Bio-Rad). Hybridization was performed as described (Bio-Rad manual). A Sph I–Pst I fragment containing the 5′-$J_{\kappa 5}$ sequence (7) was used as a probe to detect rearranged DNA (Fig. 2). For DNA sequencing, the amplified DNA's from spleen and thymus were treated with T4 DNA polymerase, and cloned into the Eco RV site of a plasmid vector, pBluescript II KS(+) (Stratagene). For cloning rearranged sequences from the brain, 1 μl of each initial PCR reaction mixture was further amplified by 25 cycles with primers 2 and 4 (Fig. 1C). The amplified DNA's were then purified and cloned into the pBluescript II KS(+) as described above.
23. For X-gal staining, transgenic mice, as well as nontransgenic littermates, were anesthetized and, when areflexic, were perfused with 1 percent glutaraldehyde and 0.5 percent paraformaldehyde in 0.1 M phosphate buffer (pH 7.4) (anesthesia procedure according to guidelines of the University of California at Berkeley). The brain was removed after 1 hour and kept in the same fixative for 4 hours. Samples for section analysis were prepared from the brain by slicing either into 2-mm slices with the rodent brain matrix (EM Corp.), or into 50-μm sections on a Vibratome. Histochemical reactions with 5-bromo-4-chloro-3-indolyl-β-D-galactoside (X-gal) were as described by Sanes *et al.* (*20*).
24. J. A. Winer, D. K. Morest, I. T. Diamond, *J. Comp. Neurol.* **274**, 422 (1988).
25. H. B. Sarnat and M. G. Netsky, *Evolution of the Nervous System.* (Oxford Univ. Press, New York, 1981).
26. J. E. LeDoux, P. Cicchetti, A. Xagoraris, L. M. Romanski, *J. Neurosci.* **10**, 1062 (1990).
27. H. Hu and A. Jayaraman, *Brain Res.* **368**, 201 (1986).
28. W. D. Neff, I. T. Diamond, J. H. Casseday, in *Handbook of Sensory Physiology, Auditory System*, W. D. Keidel and W. D. Neff, Eds. (Springer-Verlag, Berlin, 1975), vol. V/2, pp. 307–400.
29. T. A. Kost, N. Theodorakis, S. Hughes, *Nucleic Acids Res.* **11**, 8287 (1983).
30. S. Subramani, R. Mulligan, P. Berg, *Mol. Cell. Biol.* **1**, 854 (1981).

31. We thank A. J. Otsuka and R. A. Maki for critically reading the manuscript, and T. Yamamori for helpful suggestions. Supported by NIH grant AI18790 and American Cancer Society grant IM-366 (H.S.), by NIH grant NS16832 (J.A.W.), and Leukemia Society of America postdoctoral fellowship M1045 (M.M.). Part of the transgenic experiment was performed during the sabbatical leave of H.S. at the Basel Institute for Immunology, which is supported by F. Hoffmann–La Roche & Co. Ltd.

15 May 1991; accepted 22 August 1991